

## Pb layer-by-layer growth at very low temperatures

M. Jałochowski

*Institute of Physics, Maria Curie-Skłodowska University, pl. M. Curie-Skłodowskiej 1, PL-20031 Lublin, Poland*

M. Hoffmann and E. Bauer

*Physikalisches Institut, Technische Universität Clausthal, D-38678 Clausthal-Zellerfeld, Federal Republic of Germany*

(Received 19 May 1994)

We have studied the growth of ultrathin Pb films on Si(111)-(6 × 6)Au surfaces at very low temperatures by reflection high-energy electron diffraction (RHEED) and resistivity measurements. Pronounced RHEED specular beam intensity oscillations were recorded at temperatures as low as 16 K. The domain size on the surface of the growing Pb film was determined from the width of RHEED streaks. The electrical resistivity data were analyzed using the quantum size effect theory of Trivedi and Ashcroft. The mean free path of the Pb conduction electrons was determined and compared with the size of the Pb surface domains and with the size of the (6 × 6)Au substrate domains. The role of morphology and electronic structure of the Si(111)-(6 × 6)Au surface and of transient mobility during the nucleation of the growing Pb film is discussed.

### I. INTRODUCTION

In the past several years, the role of various mechanisms governing the epitaxial layer-by-layer growth mode of metal films has been discussed in many experimental and theoretical papers. Observations of reflection high-energy electron diffraction (RHEED) specular beam intensity oscillations, during metal deposition at low temperatures [Ni on W at 100 K,<sup>1</sup> Pb on Si(111) at 95 K,<sup>2</sup> and Fe and Cu on Ag (Ref. 3) at 77 K], have clearly shown that epitaxial layer-by-layer growth at temperatures below 100 K is possible.

At very low temperatures thermally activated diffusion, which is the most important factor governing the growth at elevated temperatures, is strongly suppressed or even totally excluded. In the search for other mechanisms responsible for the layer-by-layer growth mode at very low temperatures, many models have been discussed and studied theoretically.

Evans *et al.*<sup>4</sup> demonstrated that neither the traditional picture of nucleation and growth nor the model of “transient” diffusion, that is diffusion without thermal activation, is necessary to explain long-lived diffraction intensity oscillations in low-temperature epitaxial growth on fcc(100) substrates. They introduced a model in which atoms impinging on an atomically rough surface move at 0 K to lower lying adsorption sites by “downward funneling,” thus smoothing the surface. Monte Carlo simulations with the help of this funneling model for the (100) surface revealed quasi-long-lived RHEED intensity oscillations in marked contrast to the simple random immobile deposition model of Ref. 5. In another work, Evans<sup>6</sup> discussed the influence of several factors on the structure of epitaxial thin films, namely, the transient mobility, the atom dynamics during deposition and the adsorption-site geometry. All these factors led to a dramatic smoothing effect of the films. Luedtke and Landman<sup>7</sup> have per-

formed molecular-dynamics (MD) simulations employing realistic many-body embedded-atom-method interaction potentials. The simulated systems were Au atoms impinging on a Ni(001) substrate and Ni atoms impinging on a Au(001) substrate. In the first case the Stranski-Krastanov growth mode, in the second the Volmer-Weber growth mode were obtained, as expected on thermodynamical grounds.<sup>8</sup> In both cases a temperature of 300 K was assumed. In their theoretical work Sanders and DePristo<sup>9</sup> rule out the idea of a transient mobility (transient diffusion) of a metal atom on a fcc(001) metal substrate consisting of the same kind of atom during adsorption at 80 K. In another study,<sup>10</sup> Sanders *et al.* have performed MD simulations for Cu on Cu(111) at 80 K. Unlike for the deposition on fcc(001) surfaces, where 99.9% of the arriving atoms localize in the first unit cell encountered, only 67% do so for Cu(111), 21% move one unit cell, 11% travel two, and the remainder move three. Thus before incorporation at 80 K an atom can make a few short hops away from the point of impact. A similar distribution was recently obtained by Lorenzi and Ehrlich<sup>11</sup> for a smooth fcc(111) Lennard-Jones crystal. Extensive MD calculations for a Cu(111) surface with island defects at 80, 300, and 500 K were presented and thoroughly discussed by Halstead and DePristo.<sup>12</sup> They considered a 10 atom fcc(111) pyramid on Cu and Pd and concluded that at 80 K “there is zero probability that the adsorbate will adhere to the side of the unperturbed defect structure, and that, even when the pyramid structure is disrupted, fewer than 6% of the trajectories fail to reach the surface.” They state that the small ratio of the diatomic binding energy (for homoepitaxy) to the bulk cohesive energy favors layer-by-layer growth on fcc(111) surfaces, due to the downward funneling mechanism. Ross and Tringides<sup>13</sup> have observed a few weak RHEED intensity oscillations during the deposition of Ag on Si(111) at 150 K. In their experiment, a variation of

the deposition rate from 1/125 ML/s to 1/4800 ML/s did not affect the shape of the RHEED intensity vs film thickness dependence. They concluded that a nonthermal mobility mechanism was responsible for controlling the film morphology.

None of the theoretical studies except a recent study by Poelsema<sup>14</sup> attempts to describe completely the low-temperature layer-by-layer growth. Also more experimental data are needed to clarify this phenomenon.

In our previous work,<sup>2</sup> the growth of Pb on a Si(111) surface at temperatures as low as 95 K was studied. On the clean Si(111)-(7 × 7) surface, layer-by-layer growth was clearly observed after some critical thickness of Pb, on the Si(111)-(6 × 6)Au surface, even from the very beginning. In ultrathin Pb layers deposited onto the Si(111)-(6 × 6)Au surface at temperatures around 100 K quantum size effects in the electrical resistivity<sup>15</sup> and in photoelectron emission<sup>16</sup> were observed and discussed. Both experiments support the idea of layer-by-layer growth of Pb at that low temperature. The question naturally arises: is epitaxial layer-by-layer growth possible even at temperatures approaching 0 K?

In the present paper, we extend the study of the growth mode of thin films to lower temperatures by depositing Pb onto Si(111) surfaces. We observe RHEED specular beam intensity oscillations at temperatures as low as 16 K. This is the lowest temperature reported so far in the literature at which such oscillations were seen. The samples were examined in several ways: (i) the RHEED specular beam intensity oscillations were recorded during deposition at different temperatures; (ii) the profiles [full width at half maximum (FWHM's)] of the RHEED streaks were determined; (iii) the resistivity of the films was measured during growth. From these data the mean free path (MFP) of the conduction electrons was determined using the theory<sup>17</sup> of the quantum size effect (QSE).

## II. EXPERIMENT

The measurements were performed in an ultrahigh vacuum system pumped by ion and Ti sublimation pumps. The base pressure was  $8 \times 10^{-11}$  mbar. During deposition of Pb, the pressure stayed below  $2 \times 10^{-10}$  mbar. The Pb films were evaporated from Ta crucibles onto monocrystalline Si(111) substrates, with the dimensions  $18 \times 4 \times 0.6$  mm<sup>3</sup> mounted with cooled Mo clamps. The cleaning procedure previously described<sup>2</sup> which gives a (7 × 7) superstructure with good quality was used. Si wafers with 7000 Ω cm resistivity at room temperature were etched in a 19:1 mixture of 65% HNO<sub>3</sub> and 40% HF and rinsed in distilled water and methanol. Flashing for a few seconds to about 1500 K in UHV resulted in the appearance of a sharp (7 × 7) superstructure RHEED pattern. In most experiments, Si(111) with the (6 × 6)Au superstructure was used as a substrate. It was produced by deposition of about  $15 \times 10^{14}$  Au atoms/cm<sup>2</sup> on Si at room temperature [2.0 ML of Au in units of the Si(111) surface atom density or about 1.1 ML of Au(111)], fol-

lowed by short (15 sec) annealing at about 1000 K and then gradual lowering this temperature to room temperature over 7 min. Direct resistive heating was used. The substrates were cooled with a gas-flow UHV liquid helium cryostat, which allows us to hold the specimen at any temperature between 16 K and 400 K. A calibrated Si diode attached to the Cu holder near the Mo clamps was used as a temperature sensor. The temperature of the Si substrate and hence of the Pb film during deposition was corrected via the resistivity vs temperature dependence of a thick Pb film. The absolute error of the temperature was estimated to be less than  $\approx 3$  K at 16 K and  $\approx 1$  K at 70 K. A precise quartz-crystal monitor with a frequency-to-voltage converter allowed us to control the deposition of Pb with an accuracy better than 1/50 ML. The RHEED system consisted of a 15 keV electron gun with a magnetic focusing lens and deflection coils, a Faraday cup for collection of the specularly reflected electrons, and a charge coupling device (CCD) camera for recording the RHEED pattern displayed on a fluorescent screen. *In situ* resistivity measurements during film deposition were made using the method described previously.<sup>15</sup> The main advantage of this method is the capability to detect with great accuracy also the small changes of the resistance caused by factors other than the simple  $1/d$  dependence ( $d$  is the thickness of the thin film). These include phenomena related to the QSE and to periodic surface roughness variations. All data were recorded in digital form for further evaluation.

## III. RESULTS AND DISCUSSION

### A. RHEED oscillations

The thickness dependence of the specular beam intensity varies strongly with the temperature of the Si(111)-(6 × 6)Au substrate as illustrated in Fig. 1. All curves were recorded at a glancing angle of incidence of the electron beam of 0.3° in the [11 $\bar{2}$ ] azimuth of the Pb layer. The layer grew epitaxially with Pb(111) || Si(111) and Pb[11 $\bar{2}$ ] || Si[1 $\bar{1}$ 0] from the very beginning even at the lowest temperature. The evaporation rate was 0.04 ML/s. Between room temperature and 16 K dramatic changes occurred. The best developed RHEED oscillations were recorded at the lowest temperatures of the substrate, which is 16 K.

Several factors determine the shape of the RHEED oscillations. It is generally accepted that the occurrence of persistent and regular oscillations indicates ideal or quasi-ideal monolayer-by-monolayer growth. This follows from considerations within the framework of the simple kinematical diffraction theory<sup>18</sup> and also from calculations performed with the more advanced dynamical diffraction theory.<sup>19</sup> The decreasing damping of the amplitude with decreasing temperature shows that the growth front of Pb films evaporated onto Si(111)-(6 × 6)Au becomes narrower with decreasing deposition temperature, that is that the number of monolayers involved in the evolution of the growth front decreases. This unexpected result calls for an explanation which does not require thermally activated diffusion.

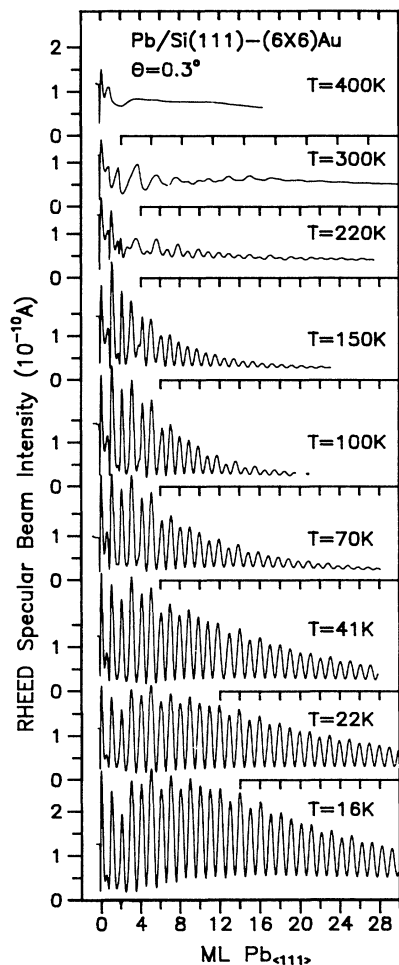


FIG. 1. Reflection high-energy electron diffraction intensity oscillations measured during the growth of Pb on Si(111)-(6 × 6)Au at different temperatures. The electron energy was 15 keV, azimuth Pb[11 $\bar{2}$ ], polar angle 0.3°. The thickness of 1 ML of Pb $_{\langle 111 \rangle}$  is 2.85 Å.

The so-called reentrant layer-by-layer growth observed experimentally with thermal-energy atom scattering (Refs. 20 and 21) for Pt on Pt(111) at temperatures above 275 K and studied theoretically<sup>22</sup> cannot be used as the proper explanation in our case. In this model thermally activated hopping is still playing a very important role. This is evident in the strong dependence of the He atom scattering intensity oscillations upon deposition rate.<sup>20</sup> With a decreasing rate, the Pt islands become larger and more regular. As a consequence, adatoms can form nuclei on top of them and three-dimensional growth begins. Such a rate dependence was not observed during the growth of Pb on Si(111)-(6 × 6)Au at 16 K. Figure 2 shows the RHEED intensity oscillations for two depositions on the same substrate at 16 K under the same conditions except for the deposition rate, which differs by a factor of 20. With an accuracy of 1.5% both plots have the same intensities and shapes. Next we discuss in detail the temperature dependence of the Pb coverage at the completion of the first monolayer as derived from the

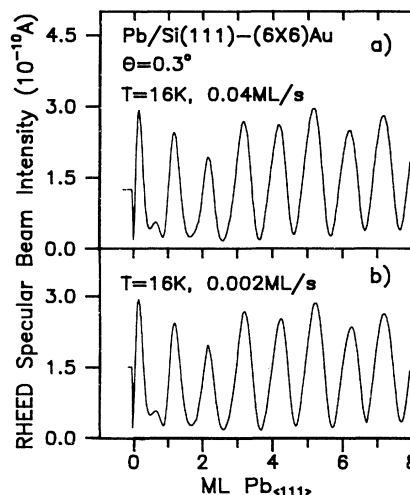


FIG. 2. Reflection high-energy electron diffraction intensity oscillations during the growth of Pb on Si(111)-(6 × 6)Au at 16 K. The deposition rate was 0.04 ML/s in case (a) and 0.002 ML/s in case (b).

thickness dependence of the RHEED intensity.

According to recent calculations, extra maxima in the reflected intensity appear during ideal monolayer-by-monolayer growth. These calculations assume that the glancing angle is very small so that the full dynamical theory can be well approximated by a one-dimensional treatment. The first theoretical results were reported by Mitura and Daniluk<sup>19</sup> and confirmed experimentally by Mitura *et al.*<sup>23</sup> for the homoepitaxy of Pb-In alloys at 110 K. In another work, Horio and Ichimiya<sup>24</sup> discussed results of calculations of RHEED intensity oscillations for Si/Si(111) homoepitaxy using the kinematical and dynamical theory of electron diffraction. A birth-death growth model was assumed in their calculations. The dynamical calculations show that at very low glancing angles, the position of a “main maximum” is not a good measure for the completion of a layer. The potential of the growing surface layer is found to play an important role in the phase of the oscillations as well as in their shape. The authors explain the origin of the extra maxima by the interference of electron waves reflected from the top and bottom faces of the growing bilayer. The phase difference of these waves depends on the potential depth of the growing layer, i.e., on the coverage of the first growing layer<sup>24</sup> and on the glancing angle. At low glancing angles (0.5°), the positions of the extra maxima correspond to the completion of growing layers. We have used these theoretical results to analyze our RHEED intensity oscillation data measured at small glancing angles in order to find out the coverage at completion of the first ML. In all plots of Fig. 1 (except in the case of 400 K), a sudden decrease of the specularly reflected electron intensity at about 1 ML thickness is clearly seen. It resembles the structure discussed in the papers cited.<sup>19,23,24</sup> Figure 3 summarizes these data. Here, the position of this decrease (taken at half of the height of the extra maximum and indicated in the inset of Fig. 3 as *s* point) is plotted

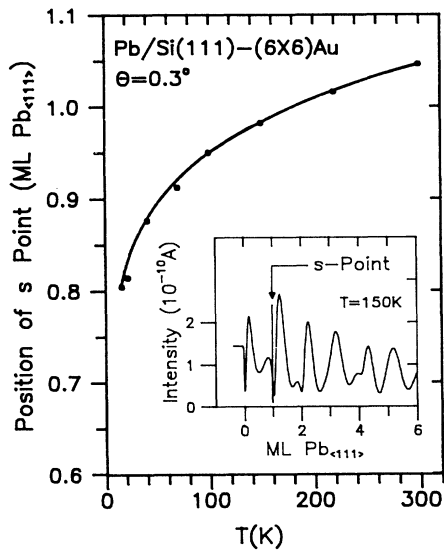


FIG. 3. The position of the  $s$  point in units of 1 ML of  $\text{Pb}_{(111)}$  as a function of the deposition temperature. Electron energy 15 keV, azimuth  $\text{Pb}[11\bar{2}]$ , polar angle  $0.3^\circ$ . The inset shows an example of the enlarged plot of the RHEED specular beam intensity variation. The solid line is a guide for the eye.

against temperature in units of 1 ML as derived from the period of the RHEED intensity oscillations in thick Pb films. The plot shows a remarkable variation of this  $s$ -point position as the substrate temperature changes. The value of 0.8 ML for the sample prepared at 16 K is an unexpected result and needs more detailed discussion.

So far calculations were made only for homoepitaxy and the influence of different substrate potentials was not considered. It also cannot be excluded that the presence of the  $(6 \times 6)\text{Au-Pb}$  interface shifts the position of the  $s$  point. On the other hand, the potential of the substrate does not change with temperature and, therefore, relative changes of the  $s$ -point position reflect the behavior of the growing film and not of the substrate. We suggest, therefore, another explanation which is based on the structure of the  $\text{Si}(111)-(6 \times 6)\text{Au}$  surface. The main feature of this surface is the modulated distribution of the Au atoms on  $\text{Si}(111)$  with the periodicity of a  $(6 \times 6)$  unit mesh. According to the models presented by Nogami *et al.*<sup>25</sup> and Dornisch *et al.*,<sup>26</sup> this periodicity is formed by a domain pattern containing a local  $(\sqrt{3} \times \sqrt{3})R30^\circ$  structure. Calculations of the electronic density of states of a  $(\sqrt{3} \times \sqrt{3})R30^\circ$  Au surface were performed by Ding *et al.*<sup>27</sup> They suggested that this surface is metallic. At a coverage of 1 ML, 75% of the Au atoms are accommodated in the  $(\sqrt{3} \times \sqrt{3})R30^\circ$  domains and 25% are built into the domain walls between them [here, 1 ML is defined by the density of Si atoms on the unreconstructed  $\text{Si}(111)$  surface,  $7.83 \times 10^{14}$  atoms/cm<sup>2</sup>]. If we assume that each Au surface atom incorporates one Pb atom, then the atomic density in the first Pb monolayer is equal to that of Si, e.g.,  $7.83 \times 10^{14}$ /cm<sup>2</sup>. This atom density corresponds to 83% of the density of a  $\text{Pb}(111)$  ML and is very close to the measured value of 80% for the position of the  $s$  point at  $T=16$  K in Fig. 3, well within

the experimental error. At this coverage the first monolayer of Pb is completed and the next arriving atoms form the second monolayer. From the analysis of the RHEED pattern, it follows that for a 4 ML thick Pb layer the lateral lattice spacing was within an accuracy of 2% of that of bulk Pb, so that the transition from the Si to the Pb packing density is completed after a few monolayers.

Now we turn to the question of which mechanism is responsible for the monolayer-by-monolayer growth at the lowest temperatures. From theoretical studies,<sup>10,12</sup> one may conclude that the transient diffusion and the funneling mechanisms may play the dominating role if the growth area is limited to only a few atomic distances. Referring to the model of the  $\text{Si}(111)-(6 \times 6)\text{Au}$  superstructure, we suggest that the size of a  $(6 \times 6)\text{Au}$  domain determines the size of a growing Pb domain. In the model developed by Nogami *et al.*<sup>25</sup> (Fig. 4), the domain walls form an array of triangular loops located equidistantly with a center separation of  $23.04 \text{ \AA}$  ( $6 \times 5.43 \text{ \AA}/\sqrt{2}$ ). The area of each loop is  $172.4 \text{ \AA}^2$ . Generally, the domain walls divide the whole  $\text{Si}(111)-(6 \times 6)\text{Au}$  surface into two regions. As mentioned above, the first region is composed of separate triangles containing a local  $\text{Au}(\sqrt{3} \times \sqrt{3})R30^\circ$  arrangement, whereas the second region, also with this superstructure but incommensurate with the first region, is the area between the triangles of the first region. Approximating the triangular domain areas by circles with the same area as indicated in Fig. 4, we obtain a mean radius of  $7.4 \text{ \AA}$ . Although transient diffusion is limited to a few interatomic distances,<sup>12</sup> it is sufficient to distribute Pb atoms in these domains. So far the theoretical studies devoted to transient diffusion phenomena considered electronically homogeneous substrates. From theoretical<sup>27</sup> and experimental<sup>25</sup> work, it follows that the surface of the  $(6 \times 6)\text{Au}$  superstructure is electronically rough also within the area of one domain. This is caused by the presence of Au trimer triplets with high electron density within the domain. We believe that they play the role of the nuclei during deposition at very low temperatures. In our model, both domain walls<sup>25</sup> and Au trimer triplets<sup>26</sup> play the role of sinks for arriving Pb atoms.

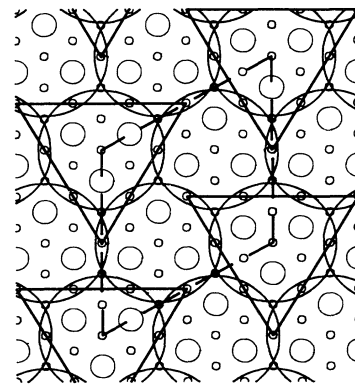


FIG. 4. Approximation of the triangular domains of the  $\text{Si}(111)-(6 \times 6)\text{Au}$  structure by circular regions. The circles with increasing size indicate Si atoms, Au trimers, and circular regions. The dashed line outlines a single  $(6 \times 6)$  unit cell and the black lines show the domain walls (Ref. 25).

In order to check how the modification of the Si(111) surface by Au adsorption influences the growth mode, we also studied the growth of Pb on the Si(111)-(7 × 7) surface. Figure 5 shows the specular beam intensity oscillations recorded during the growth of Pb on the Si(111)-(7 × 7) at two different temperatures. The damping of the oscillations beyond about 5 ML is very similar to that on the Si(111)-(6 × 6)Au surface (Fig. 1), at least at low temperatures, which indicates very similar growth in spite of completely different initial growth. As reported previously,<sup>2</sup> Pb grows on this substrate at 95 K with Pb(111) ∥ Si(111) and Pb[11 $\bar{2}$ ] ∥ Si[11 $\bar{2}$ ]. This was confirmed by Weitering *et al.*<sup>28</sup> during their low-energy electron diffraction and RHEED experiments at room temperature, which showed that the first monolayer forms a two-dimensional adlayer of Pb atoms, occupying a lattice of 8 × 8 sites per 7 × 7 surface unit cell. This monolayer is highly compressed with a 4.2% change of the Pb-Pb distance. During deposition onto cooled substrates, we found an amorphouslike initial growth mode. This was clearly seen in the RHEED patterns, where no streaks could be observed but only strong background. The phase transition into the crystalline state occurred after some critical thickness. This was visible in the sudden appearance of the Pb diffraction streaks in the RHEED pattern. The critical thickness, which is marked with an asterisk in Fig. 5, increased with decreasing temperature. At 70 K it was 4 ML, at 18 K 7 ML. The absence of the amorphous layer on the (6 × 6)Au superstructure indicates that the interaction between Pb and the Au-saturated surface is much stronger than between Pb and the clean Si surface forcing crystalline growth from the very beginning. Thus, Au acts as an “interfacant,” which differs from a surfactant by remaining localized at the interface during growth.

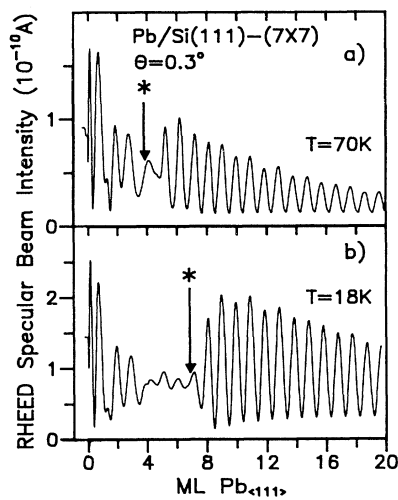


FIG. 5. Reflection high-energy electron diffraction intensity oscillations during the growth of Pb on Si(111)-(7 × 7). Electron energy 15 keV, azimuth Pb[11 $\bar{2}$ ], polar angle 0.3°. The temperature of the substrate was 70 K in (a), and 18 K in (b). The asterisk denotes the Pb film thickness at which the streaks in the RHEED pattern appeared.

We turn once more to Fig. 3 to discuss the temperature dependence of the position of the *s* point. If the saturation occupation of the first Pb monolayer on the (6 × 6)Au surface does not depend on temperature, then it follows from Fig. 3 that at about 180 K, 0.2 ML of Pb is already in the second and in the next monolayers when the first monolayer is completed. At 300 K, an even larger amount of Pb occupies the higher layers before completion of the first monolayer. This is consistent with the observed strong temperature-dependent damping of the RHEED oscillations. Apparently the monolayer-by-monolayer growth mode at the lowest temperatures converts into three-dimensional growth at elevated temperatures. This is simply a manifestation of the thermally activated mobility on the growing Pb surface, which leads to the formation of larger two-dimensional islands. In such circumstances the growth is not limited by short-range transient diffusion any longer and with increasing temperature a slow and steady change of the growth mode occurs.

Finally, we briefly discuss the visible 2 (or near 2) ML modulation of the RHEED intensity oscillations (e.g., Fig. 1). Similar to our previous work,<sup>15</sup> we regard these as the manifestation of the QSE in the reflection of energetic electrons. This effect is rather temperature independent. Although the amplitude of the 1 ML oscillations changes dramatically over the temperature range from 16 K to 220 K the absolute value of the modulation with 2 ML periodicity is almost constant. This behavior can be understood if we realize that with an increase of temperature the number of monolayers involved in the evolution of the growth front changes from 1 ML gradually into 2 ML, 3 ML, or even more. As a consequence, the surface roughness oscillations causing the 1 ML periodic oscillations of the RHEED specular beam intensity and the electrical resistivity will be lost earlier than the oscillations of 2 ML periodicity characteristic of QSE. Such a behavior was also clearly evident in our previous works devoted to the study of the QSE in ultrathin Pb films.<sup>15</sup> We were able to explain the appearance of both 1 and 2 ML structures using a simple growth model and without invoking a growth model in which simultaneous growth of 2 Pb ML has been assumed.<sup>29</sup>

## B. Size of the Pb domains

In the model of the layer-by-layer growth considered here, the size of a domain which confines the area of the transient diffusion plays an important role. In order to determine this size, we used two independent experimental methods.

The measurement of the FWHM of the RHEED streaks is a straightforward and surface sensitive method, which allows us to estimate the domain size. The experimental data for the [01] rod in the Pb[11 $\bar{2}$ ] azimuth at a polar angle of 0.6° were corrected by deconvolution of the instrumental broadening and the mean size  $D = a_{0\text{Pb}}/(2\sqrt{2}\Delta k)$  was calculated, with  $\Delta k$  being the

FWHM in units of the reciprocal lattice vector  $g_{[10]}$ . The results are presented in Table I.

A volume sensitive method, which gives information on the domain size, is the *in situ* measurement of the specific resistivity and its analysis within the framework of the QSE theory.<sup>17</sup> The method was recently thoroughly discussed by Jałochowski *et al.*<sup>15</sup> and it was stressed that this theory allows a quantitative description of the dependence of the specific resistivity upon film thickness. This is extremely important for films with a thickness of only a few monoatomic layers, for which the application of the classical Fuchs-Sondheimer theory is no longer justified and may lead to incorrect conclusions.<sup>15</sup> Figure 6 shows the experimental data of the specific resistivity measurements of Pb films deposited on cooled Si(111)-(6×6)Au substrates. Similar to the data presented previously two periods are seen in the variation of the specific resistivity  $\rho$ . They are more evident in  $d\rho/dd$  plots obtained by numerical differentiation of the  $\rho(d)$  curve as illustrated for the 18 K deposition. The 2 ML periodicity is caused by the size quantization of the energy band structure, while the 1 ML periodicity results from the periodic variation of the surface roughness during monolayer-by-monolayer growth. Both effects were explained in our earlier work with the theory of Trivedi and Ashcroft.<sup>17</sup> According to this theory the specific conductivity  $\sigma$  is given by

$$\sigma = \frac{e^2 k_F}{\hbar \pi^2} \frac{1}{\kappa} \sum_{n=1}^{n_c} \frac{1 - n^2/\kappa^2}{\frac{2n_c+1}{k_F l \kappa} + \left(\frac{\delta d}{d}\right)^2 \frac{s(n_c)n^2}{3\kappa}}, \quad (1)$$

where  $k_F$  is the Fermi wave vector,  $\kappa = k_F d/\pi$ ,  $n_c = \text{Int}(\kappa)$ ,  $s(n_c) = (2n_c + 1)(n_c + 1)n_c/(3\kappa^3)$ , and  $l$  is the MFP.  $\delta d$  describes the small-scale roughness and is the root-mean-square deviation of the mean film thickness  $d$ . Expression (1) is a complete description of both volume

TABLE I. The FWHM  $\Delta k$  of the [01] rod in units of the reciprocal lattice vector  $g_{[01]}$ , the resulting mean domain size  $D$ , the experimental specific resistivity data  $\rho_{\text{exp}}$ , the temperature-dependent specific resistivity  $\rho_{\text{ph}}$  (Ref. 31), and the mean free path  $l$  calculated from Eq. (4) together with Eq. (5).  $T$  (K) means the substrate temperature during the deposition of Pb and during the measurements.

RHEED measurement ( $d = 5$ ML)			
$T$ (K)	$\Delta k$ ( $g_{[01]}$ )	$D$ (Å)	
16	0.116	15.1	
22	0.135	13.0	
41	0.112	15.6	
67	0.102	17.2	
100	0.065	26.9	
150	0.056	31.3	
220	0.051	34.3	
300	0.037	47.3	
Resistivity measurement ( $d = 5$ ML)			
$T$ (K)	$\rho_{\text{exp}}$ ( $\mu\Omega$ cm)	$\rho_{\text{ph}}$ ( $\mu\Omega$ cm)	$l$ (Å)
18	31.5	0.40	17.2
32	34.0	1.5	16.5
50	30.6	2.8	19.3
70	31.0	4.3	20.1
140	33.8	9.4	22.0

and surface electron scattering contributions influenced by the quantum size effect. As noted in the work of Trivedi and Ashcroft<sup>17</sup> the total rate of electron scattering is additive. However, the total resistivity is not given by a sum of the impurity and surface resistivities, i.e., Matthiessen's rule is not obeyed. Expression (1) can be simplified considerably if we assume that the small-scale roughness  $\delta d$  can be neglected for thin films consisting of an integer number of monoatomic layers. It is certainly true for 5 ML thick Pb films because the RHEED intensity oscillations are very well developed in this coverage range. Taking  $\delta d = 0$ , we obtain the expression

$$\sigma = \sigma_D 3 \sum_{n=1}^{n_c} \frac{1 - n^2/\kappa^2}{2n_c + 1}, \quad (2)$$

where

$$\sigma_D = \frac{e^2 k_F^2 l}{3\pi^2 \hbar} \quad (3)$$

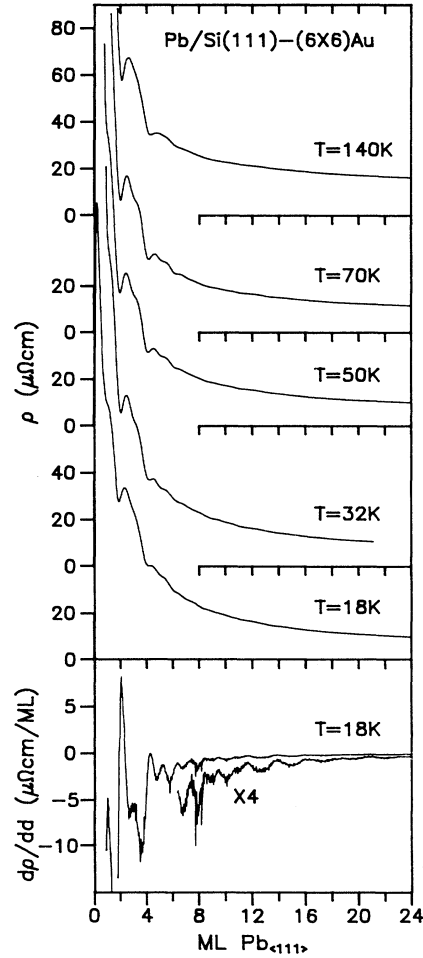


FIG. 6. Specific electrical resistivity of the growing Pb film on a Si(111)-(6×6)Au substrate as a function of film thickness. For the sample deposited at 18 K, the numerically calculated specific resistivity derivative  $d\rho/dd$  is shown. Note the presence of oscillations with 1 ML period and a 2 ML modulation.

is the Drude conductivity. The wave vector  $k_F = 1.6062 \text{ \AA}^{-1}$  is obtained by fitting the energy dependence  $E = \hbar^2 k^2 / (2m^*)$  to the experimental data of Fig. 11 in Ref. 30. The correction of the volume specific conductivity caused by the presence of QSE effects for a sample with a particular thickness can be calculated from equation (2) and yields for samples with thicknesses of  $d = 5 \text{ ML}$ ,

$$\sigma = 0.872 \sigma_D . \quad (4)$$

In contrast to Eq. (1), expression (4) obeys Matthiessen's rule and can, therefore, be used to calculate the MFP  $l$  from the experimental resistivity data after subtraction of the temperature dependent contribution to the specific resistivity caused by phonon scattering. Our experimental data  $\rho_{\text{exp}}$  presented in Table I were analyzed according to Eq. (4). First  $\rho_{\text{exp}}$  was separated into the well known  $\rho_{\text{ph}}$  due to temperature-dependent phonon scattering<sup>31</sup> and  $\rho_0$  due to temperature-independent scattering so that

$$\rho_0 = \rho_{\text{exp}} - \rho_{\text{ph}} . \quad (5)$$

The  $\rho_0 = 1/\sigma$  values obtained from Eq. (5) were used to calculate  $\sigma_D$  in Eq. (4) and the mean free path  $l$  that is not due to the phonon scattering was finally obtained from Eq. (3). The calculation of  $l$  was restricted to samples deposited at temperatures below 150 K because at higher temperatures the growth mode of the Pb films changes into a more three-dimensional one as is evident from the RHEED oscillation data presented in Fig. 1. Obviously such "high-temperature" grown films cannot be described by Eq. (4), which assumes an atomically smooth surface. The results of the calculation of the MFP  $l$  of 5 ML thick films are summarized together with the  $D$  values from the RHEED measurements in Table I and are displayed in Fig. 7. Although the theory of Trivedi and Ashcroft describes a thin film at 0 K, we believe that it is still applicable in our situation. This is because of the large separation of the QSE energy levels in samples with 5 ML thickness. As is evident from our

previous work,<sup>16</sup> this separation is more than 0.5 eV at the Fermi level and is well above the thermal smearing.

The MFP's determined from the specific resistivity measurements and the parameter  $D$  from the RHEED streak profile measurements can be regarded as a measure of the domain size. They reflect the surface and volume morphology of the growing film. Extrapolation to 0 K gives a value of about 12 Å for  $D$  and about 15 Å for  $l$ . These values are very close to the mean size of the domains (14.8 Å of diameter) forming the  $(6 \times 6)\text{Au}$  superstructure<sup>25</sup> (Fig. 4). Small average island distances and island sizes are a common feature of metallic thin films deposited at low temperatures. Bott *et al.*<sup>32</sup> studied with STM the morphology of Pt evaporated on Pt(111) at temperatures down to 205 K. In their experiment, the average island distance changes remarkably from 1700 Å at 628 K to 87 Å at 205 K. Simultaneously, the shape of the island varied from large triangles to fractal-like small aggregates. In another study Röder *et al.*<sup>33</sup> have found that Ag deposited on Pt(111) at 25 K nucleated as single isolated adatoms. In their STM experiment clustering into small two-dimensional islands was observed above 40 K. Strocio *et al.*<sup>34</sup> observed in their STM images homoepitaxial growth of Fe on Fe(001) whiskers. At 293 K, where weak RHEED oscillations were still visible, they found that the average island distance was about 50 Å.

A film growing at very low temperatures is far from equilibrium and has the tendency to transform into a more ordered structure. The MFP's determined for 20 ML thick films were three times larger than for 5 ML thick films. Apparently, with increasing film thickness, the domain size increases. This makes the transient diffusion mechanism ineffective and the layer-by-layer growth is destroyed, which leads to the damping of the RHEED intensity oscillations. Due to the increased thermal mobility at higher temperatures, larger domains are formed and the transition to three-dimensional growth occurs.

#### IV. SUMMARY

Reflection high-energy electron diffraction intensity oscillations and electrical resistivity measurements confirmed in detail the monolayer-by-monolayer growth of Pb on a Si(111)-(6 × 6)Au surface at very low temperatures. The damping of RHEED intensity oscillations decreased with decreasing temperature and the best developed oscillations were seen at 16 K, the lowest temperature reached.

To explain this phenomenon we invoke transient mobility, which may play the most important role in the case when thermally activated diffusion is suppressed. So far none of the theoretical studies devoted to thin film growth at temperatures approaching 0 K have discussed the influence of other physical factors such as modulation of the surface crystal potential by surface reconstruction [as in the case of the  $(6 \times 6)\text{Au}$  superstructure] and the presence of domain walls. We have shown that these causes have to be taken into account. The domain sizes  $D$  of a 5 ML thick Pb film determined from the RHEED diffraction streak profile were close to the  $(6 \times 6)\text{Au}$  do-

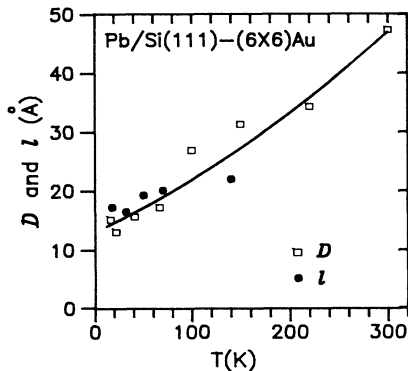


FIG. 7. Temperature dependence of the domain size  $D$  determined from the RHEED profile measurements and the mean free path  $l$  of the conduction electrons calculated from the specific resistivity data for a 5 ML thick Pb layer. The solid line is a guide for the eye.

main sizes. Extrapolated to 0 K, they were about 13 Å.

In the second type of experiments, the specific resistivity of the growing Pb film was measured. In order to determine the value of the MFP of the conduction electrons, the QSE theory of the electrical resistivity was used. The temperature-independent component of the mean free path, due to volume scattering and not to phonon scattering, for a 5 ML thick sample extrapolated to 0 K deposition temperature was about 15 Å.

The values of  $D$  and of the MFP are in good agreement with the  $(6 \times 6)$ Au superstructure domain size proposed by Nogami *et al.*<sup>25</sup> In their model, the  $(6 \times 6)$ Au superstructure is composed of  $(\sqrt{3} \times \sqrt{3})R30^\circ$  regions enclosed by Au-rich domain walls. Dornisch *et al.*<sup>26</sup> describe these domains as an arrangement of Au trimer triplets. In their study, the domain walls are also described as regions with higher Au atom density separating  $(\sqrt{3} \times \sqrt{3})R30^\circ$  regions.

To explain the experimental data, we propose that the

Au trimer triplets and domain walls are playing the role of nucleation centers. In this picture, the regular distribution of the trimer triplets within one domain determines the structure and the crystallite size of the Pb film in the early stage of growth at very low temperatures. The limited range transient mobility causes a homogeneous distribution of the impinging Pb atoms on this small crystallite. At higher temperatures the crystallites tend to grow in size so that the limited transient mobility range cannot assure Pb adatom transport to the step edges. This manifests itself in an increasing damping of the RHEED intensity oscillations and also in a smoothing of the thickness dependence of the specific resistivity.

#### ACKNOWLEDGMENTS

This work was supported by the Deutsche Forschungsgemeinschaft and by Grant No. 2-0382-91-01 of the Polish Committee of Scientific Research.

- 
- <sup>1</sup> C. Koziol, G. Lilienkamp, and E. Bauer, *Appl. Phys. Lett.* **51**, 901 (1987).  
<sup>2</sup> M. Jałochowski and E. Bauer, *J. Appl. Phys.* **63**, 4501 (1988).  
<sup>3</sup> W. F. Egelhoff, Jr. and I. Jacob, *Phys. Rev. Lett.* **62**, 921 (1989).  
<sup>4</sup> J. W. Evans, D. E. Sanders, P. A. Thiel, and Andrew E. DePriesto, *Phys. Rev. B* **41**, 5410 (1990).  
<sup>5</sup> J. W. Evans, *Phys. Rev. B* **39**, 5655 (1989).  
<sup>6</sup> J. W. Evans, *Phys. Rev. B* **43**, 3897 (1991).  
<sup>7</sup> W. D. Luedtke and Uzi Landman, *Phys. Rev. B* **44**, 5970 (1991).  
<sup>8</sup> E. Bauer, *Z. Kristallogr.* **110**, 372 (1958).  
<sup>9</sup> D. E. Sanders and A. E. DePriesto, *Surf. Sci.* **254**, 341 (1991).  
<sup>10</sup> D. E. Sanders, D. M. Halstead, and A. E. DePriesto, *J. Vac. Sci. Technol. A* **10**, 1986 (1992).  
<sup>11</sup> G. De Lorenzi and G. Ehrlich, *Surf. Sci. Lett.* **293**, L900 (1993).  
<sup>12</sup> D. M. Halstead and A. E. DePriesto, *Surf. Sci.* **286**, 275 (1993).  
<sup>13</sup> K. R. Ross and M. C. Tringides, *Phys. Rev. B* **47**, 12 705 (1993); *Surf. Sci.* **302**, 37 (1994); *Europhys. Lett.* **23**, 257 (1993).  
<sup>14</sup> B. Poelsema (unpublished).  
<sup>15</sup> M. Jałochowski and E. Bauer, *Phys. Rev. B* **38**, 5272 (1988); M. Jałochowski, E. Bauer, H. Knoppe, and G. Lilienkamp, *ibid.* **45**, 13 607 (1992).  
<sup>16</sup> M. Jałochowski, H. Knoppe, G. Lilienkamp, and E. Bauer, *Phys. Rev. B* **46**, 4693 (1992).  
<sup>17</sup> N. Trivedi and N. W. Ashcroft, *Phys. Rev. B* **38**, 12 298 (1988).  
<sup>18</sup> P. I. Cohen, G. S. Petrich, P. R. Pukite, G. J. Whaley, and A. S. Arrott, *Surf. Sci.* **216**, 222 (1989).  
<sup>19</sup> Z. Mitura and A. Daniluk, *Surf. Sci.* **277**, 229 (1992).  
<sup>20</sup> R. Kunkel, B. Poelsema, L. K. Verheij, and G. Comsa, *Phys. Rev. Lett.* **65**, 733 (1990).  
<sup>21</sup> B. Poelsema, A. F. Becker, G. Rosenfeld, R. Kunkel, N. Nagel, L. K. Verheij, and G. Comsa, *Surf. Sci.* **272**, 269 (1992).  
<sup>22</sup> P. Smilauer, M. R. Wilby, and D. D. Vvedensky, *Phys. Rev. B* **47**, 4119 (1993).  
<sup>23</sup> Z. Mitura, M. Stróžak, and M. Jałochowski, *Surf. Sci. Lett.* **276**, L15 (1992).  
<sup>24</sup> Y. Horio and A. Ichimiya, *Surf. Sci.* **298**, 261 (1993).  
<sup>25</sup> J. Nogami, A. A. Baski, and C. F. Quate, *Phys. Rev. Lett.* **65**, 1611 (1990).  
<sup>26</sup> D. Dornisch, W. Moritz, H. Schulz, R. Feidenhans'l, M. Nielsen, F. Grey, and R. L. Johnson, *Phys. Rev. B* **44**, 11 221 (1991).  
<sup>27</sup> Y. G. Ding, C. T. Chan, and K. M. Ho, *Surf. Sci. Lett.* **275**, L691 (1992).  
<sup>28</sup> H. H. Weitering, D. R. Heslinga, and T. Hibma, *Phys. Rev. B* **45**, 5991 (1992).  
<sup>29</sup> B. J. Hinch, C. Koziol, J. P. Toennies, and G. Zhang, *Vacuum* **42**, 309 (1991).  
<sup>30</sup> R. C. Jaklevic and J. Lambe, *Phys. Rev. B* **12**, 4146 (1975).  
<sup>31</sup> G. T. Meaden, *Electrical Resistance of Metals* (Plenum Press, London, 1965).  
<sup>32</sup> M. Bott, T. Michely, and G. Comsa, *Surf. Sci.* **272**, 161 (1992).  
<sup>33</sup> H. Röder, H. Brune, J. Bucher, and K. Kern, *Surf. Sci.* **298**, 121 (1993).  
<sup>34</sup> J. A. Stroschio, D. T. Pierce, and R. A. Dragoset, *Phys. Rev. Lett.* **70**, 3615 (1993).